P&O MAXIMUM POWER POINT REGULATION MODEL FOR TWO STAGE GRID CONNECTED PV SYSTEMS

Mihai IONESCU[1]

The starting point of this work is represented by an accurate model of a 247 kWp photovoltaic system based on the simple exponential model. The evolution of the maximum power output and maximum power point voltage in variable temperature and solar irradiance conditions is being followed. Perturb and Observe (P&O) maximum power point regulation model is created using Matlab® Simulink Simscape components, in order to provide a closer look to the physical process involving the Pulse Width Modulated (PWM) command of a BOOST DC-DC converter. The developed model is used for optimal tuning of P&O maximum power point regulator, considering fast variable solar irradiance conditions.

Keywords: PV system, Perturb and Observe, BOOST converter, maximum power point, PWM

1. Introduction

During the last couple of decades, photovoltaic technologies experienced a very fast market development, so the interest of improving the efficiency of newly installed capacities is constantly increasing. Therefore, specialized literature is abundant in maximum power point tracking techniques (MPPT), proposing an impressive number of principles characterized by different complexity, efficiency, speed of operation and application cost ranges [1], [2], [8].

In present, the most frequently used maximum power point regulation technique for medium and large PV systems is the P&O method. Although it is characterized by a series of limitations, such as permanent oscillations around the maximum power point and temporary divergence in fast solar irradiance variation conditions, the ease of implementation and cost effectiveness are consistent arguments to use P&O maximum power point tracking method on a wide scale.

Considering the case of two stage conversion PV systems, the maximum power point output regulator is represented by a DC-DC converter. Taking into account the fact that in most cases the necessary input voltage for the grid interface inverter is higher than the PV system output voltage, it can be concluded that the BOOST DC-DC converter is the most frequently used in two stage conversion PV systems applications.

[1] PHD student of Automatic and Computer Science Faculty, University POLITEHNICA of Bucharest, Romania, e-mail: mihaiandrei.ionescu@gmail.com

This paper provides P&O maximum power point regulation model for two stage conversion grid-connected PV systems, involving also a high accuracy PV system model in variable temperature and solar irradiance conditions. The behavior of maximum power point regulation is analyzed considering an entire characteristic day temperature and solar irradiance measurements in order to highlight the advantages and limitations of this technique.

2. Theoretical aspects

The P&O algorithms involve continuous measurement of the PV system's output voltage V_{PV} and current I_{PV}. It operates by periodically perturbing the PV array's output voltage and analyzes the response of the output power to that perturbation. If the obtained output power increases as consequence of voltage modifying, the next perturbation cycle will vary the output voltage in the same direction as the previous one. If the output power decreases during the last perturbation cycle, the next perturbation cycle will vary the PV array's output voltage in the other direction.

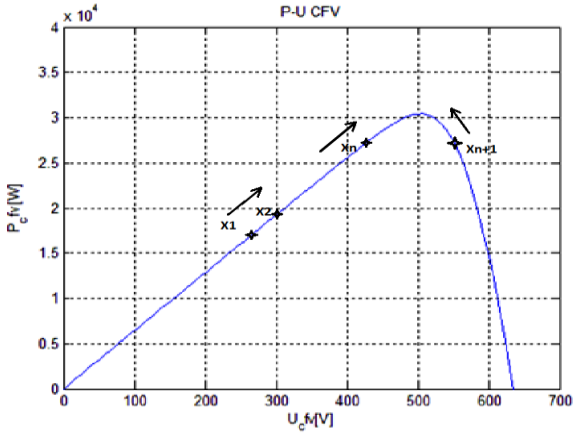

Fig.1. Operating principle of the P&O algorithm

The advantages of P&O algorithms are simplicity and ease of implementation. However, this method encounters a series of limitations that may affect the PV system's energy efficiency. A common problem in P&O algorithms is that the array terminal voltage is perturbed every MPPT cycle; therefore, when the MPP is reached, the output power oscillates around the maximum, resulting in power loss in the PV system. This aspect is more obvious in slowly variable solar irradiance and temperature conditions. In order to reduce power losses, the size of the perturbation produced by P&O algorithm should be reduced. Unfortunately, this solution would decrease convergence speed of the algorithm.

A second limitation is provided by the fact that in rapidly changing solar irradiance conditions, P&O algorithms may become unstable [2]. Considering the PV array operating point is *X1 (Fig. 1)*, on the first *P-U* curve, a sudden increase of light irradiance would move the operating point to *X2*, on the second *P-U* curve. In this case, the algorithm detects an output power increase and continues to increase voltage during the next perturbation cycle. On the other hand, if the operating point of the PV system is *X3*, on the second *P-U* curve, a sudden decrease of solar irradiance would move the operating point to *X4*, on the first *P-U* curve. In this case, the algorithm detects an output power decrease and decreases the output voltage during the next perturbation cycle.

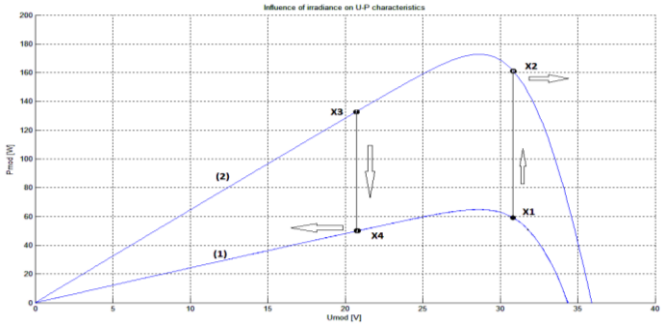

Fig.2. Temporary divergence of P&O algorithm during fast solar irradiance variations

3. PV system model approach

The PV system considered for this study consists in 1152 modules connected in 72 strings. Each module consists in 60 PV cells series connected and has a rated power of 215 Wp. The input data of the model is represented by parameters measured in Standard Test Conditions during factory acceptance tests: the short circuit current I_{sc}, the open circuit voltage U_{oc}, the maximum power point voltage U_m, the maximum power point current I_m and the maximum power P_m. PV model approach is based on the simple exponential model, written for each module, described by equations *(1)* and *(2)* [8].

$$I = I_{ph} - I_{0d} \cdot (e^{\frac{U + R_s \cdot I}{V_t}} - 1) - \frac{U + R_s \cdot I}{R_{sh}} \tag{1}$$

$$V_t = 60 \cdot \frac{n \cdot k \cdot T}{q} \tag{2}$$

where:

- ✓ I_{ph} is the photocurrent [A];
- ✓ I_{0d} is the saturation current of the junction [A];
- ✓ R_s is the series resistance [Ω];
- ✓ R_{sh} is the parallel resistance (or shunt resistance) [Ω];

- ✓ V_t is the thermal voltage gap [V];
- ✓ n is the quality factor of the p-n junction [-];
- ✓ q is the elementary charge ($1.602 \cdot 10^{-19}$ C);
- ✓ k represents the Boltzmann constant ($1.38 \cdot 10^{-23}$ J/K);
- ✓ T is the cell's absolute temperature [K].

Considering the fact that the equation describing the PV system I-U characteristic cannot be used in Matlab® Simulink tool, the PV model approach consists in two distinct stages. The first stage is an equivalent scheme parameters computing algorithm for variable temperature and solar irradiance conditions. The second stage involves PV system *I-U* characteristic determination for specific measured values of temperature and solar irradiance. The output necessary data of the equivalent scheme parameters computing algorithm is represented by the photocurrent I_{ph},the saturation current I_{0d}, the series resistance R_s, the parallel resistance R_{sh} and the quality factor n, calculated for each module. Writing the simple exponential model equation for maximum power point, open circuit and short circuit conditions and considering the maximum power point condition are obtained equations *(3)-(6).*

$$I_{sc} = I_{ph} - I_{0d} \cdot (e^{\frac{R_s \cdot I_{sc}}{V_t}} - 1) - \frac{R_s \cdot I_{sc}}{R_{sh}} \tag{3}$$

$$0 = I_{ph} - I_{0d} \cdot (e^{\frac{U_{oc}}{V_t}} - 1) - \frac{U_{oc}}{R_{sh}} \tag{4}$$

$$I_m = I_{ph} - I_{0d} \cdot (e^{\frac{U_m + R_s \cdot I_m}{V_t}} - 1) - \frac{U_m + R_s \cdot I_m}{R_{sh}} \tag{5}$$

$$\left(\frac{\partial P}{\partial U}\right)_{MPP} = 0 \tag{6}$$

Considering the fact there is available measured data for each model, a statistic estimation can be assumed for the quality factor n, following a normal distribution, as shown in *Fig. 3*.

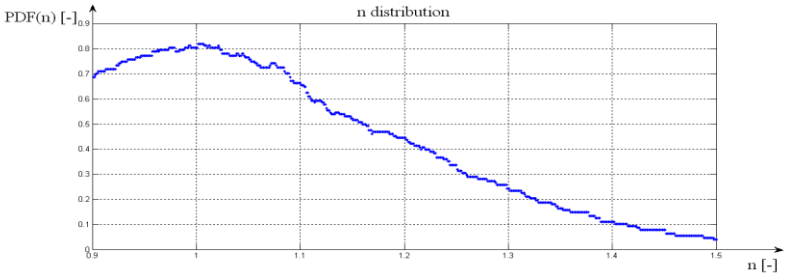

Fig.3 - Quality factor distribution in Standard Test Conditions

By this approach, the problem is reduced to a determined system of equations that can be solved using the bisection method.

In order to obtain PV model's parameters for different temperatures, it must be taken into account that input data variation with temperature is described in equations *(7), (8)* and *(9),* where coefficients α_I, β_V and γ_P represent catalog data provided by the PV modules' manufacturer. For every temperature considered in this study, a normal distribution for the quality factor *n* had to be approximated, as shown in *Fig. 4.* The calculations are being performed for temperatures between -10°C and 70°C with an increment step of 5°C.

$$I_{sc} = I_{sc\_STC} \cdot (1 + \alpha_I \cdot \Delta T) \tag{7}$$

$$U_{oc} = U_{oc\_STC} \cdot (1 + \beta_V \cdot \Delta T) \tag{8}$$

$$P_m = P_{m\_STC} \cdot (1 + \gamma_P \cdot \Delta T) \tag{9}$$

where:

- ✓ U_{oc_STC} is the open circuit voltage in Standard Test Conditions;
- ✓ I_{sc_STC} is the short circuit current in Standard Test Conditions;
- ✓ α_I, β_V are the current, respectively the voltage coefficients;
- ✓ P_{max_STC} is the maximum output power in Standard Test Conditions;
- ✓ γ_P is the power coefficient and it is negative.

In order to obtain PV model's parameters for different values of solar irradiance, determination of the three base points on the *I-U* characteristic is necessary. Considering the simplified short circuit condition expressed in equation *(10)* and the fact that the photocurrent increases linearly with solar irradiance, it can be concluded that the short circuit current also increases linearly with solar irradiance. The constant k can be determined from standard test conditions results.

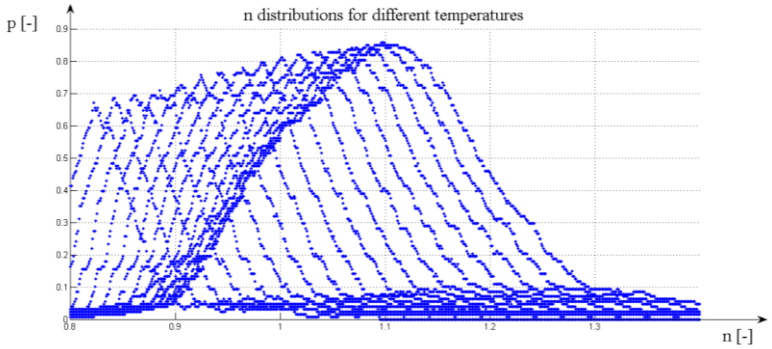

Fig.4. The quality factor distributions for the considered temperature range

$$I_{sc} = I_{ph} \tag{10}$$

$$I_{ph} = k \cdot G \tag{11}$$

$$I_{sc} = k \cdot G \tag{12}$$

Knowing that the saturation current I_{0d} and the quality factor n are invariable with solar irradiance, equation *(13)* depending on the open circuit voltage U_{oc} and the shunt resistance R_{sh} is obtained from the open circuit condition. Specialized literature [3] provides the variation of maximum power point coordinates with solar irradiance described in equations *(14)* and *(15)*.

$$0 = I_{ph} - I_{0d} \cdot (e^{\frac{U_{oc}}{V_t}} - 1) - \frac{U_{oc}}{R_{sh}} \tag{13}$$

$$I_m = I_{m\_STC} \cdot \frac{G}{G_{STC}} \tag{14}$$

$$0 = I_{ph} - I_{0d} \cdot (e^{\frac{U_{oc}}{V_t}} - 1) - \frac{U_{oc}}{R_{sh}} \tag{15}$$

By this, three independent equations are obtained, and three unknown parameters: the open circuit voltage U_{oc}, the series resistance, R_s and the shunt resistance R_{sh}. The equivalent scheme parameters computing is performed considering a solar irradiance interval between 300 and 1200 W/m^2, with an increment step of 100 W/m^2. Taking into account the fact that the equivalent scheme parameters computing algorithm provides very low disperses between the modules composing the PV system, it can be considered that the PV system consists in identical modules with parameters calculated as average. In this case, the equivalent parameters of the entire PV system are described by equations *(16)* - *(19)*.

$$I_{ph\_ech} = n_p \cdot I_{ph\_average} \tag{16}$$

$$I_{0d\_ech} = n_p \cdot I_{0d\_average} \tag{17}$$

$$R_{s\_ech} = \frac{n_s}{n_p} \cdot R_{s\_average} \tag{18}$$

$$R_{sh\_ech} = \frac{n_s}{n_p} \cdot R_{sh\_average} \tag{19}$$

where:

- ✓ n_s represents the number of series connected PV modules;
- ✓ n_p represents the number of series connected PV modules.

The results of this algorithm can be stored in five 17x10 matrix databases.

For *I-U* characteristics determination is chosen a characteristic day with variable nebulosity, involving fast solar irradiance variations. Temperature and solar irradiance measurements are performed during a day, between 8:00 and 20:00, delayed one from each other by a 10 minutes time interval, resulting in 72 measurement points. For simplification, the measured values are considered constant during each 10-minutes time interval and are centralized in the graphs shown in *Fig. 5*. Taking into account the equivalent scheme parameters databases exampled by *Table 1*, it can be considered that each parameter can be written as a function dependant on temperature and solar irradiance. By this approach, determination of *I-U* characteristics for each measurement point is reduced to a bilinear interpolation for each parameter, described by equations *(20)* - *(22)*.

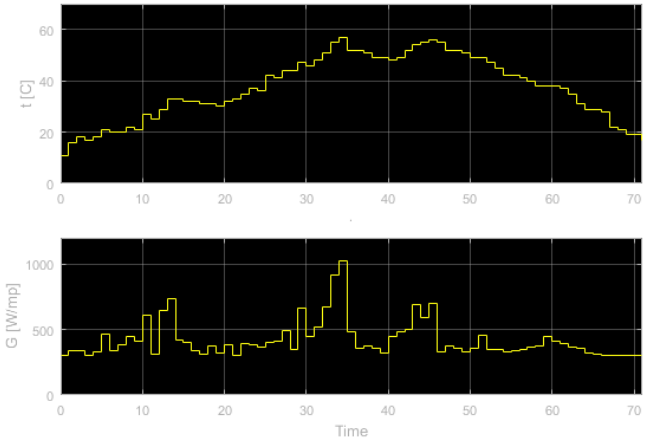

Fig.5. Temperature and solar irradiance evolution during the characteristic day

$$R_s = f(T_{meas}, G_{meas}) \tag{20}$$

$$T_{meas} \in [T_i, T_{i+1}] \tag{21}$$

$$G_{meas} \in [G_i, G_{i+1}] \tag{22}$$

where:

- ✓ T_{meas} and G_{meas} represent measured values of the temperature, respectively the irradiance for a specific time;
- ✓ T_i, T_{i+1} are consecutive temperature values for which was applied the equivalent scheme parameters computing algorithm;
- ✓ G_i, G_{i+1} are consecutive solar irradiance values for which was applied the equivalent scheme parameters computing algorithm.

By this approach, the *I-U* characteristics can be calculated for each measured values of temperature and solar irradiance and stored in databases. The characteristics are calculated considering a voltage variation between 0 and 800

V, with increment step of 1 V. It results in a 72x801 matrix database for the considered *I-U* characteristics.

4. Maximum power point regulation model implementation

The Perturb and Observe maximum power point regulation algorithm is implemented by PWM command of a BOOST DC-DC converter as shown in *Fig. 6*. PV system model is applied using a controlled current source using as input data the *I-U* characteristics database.

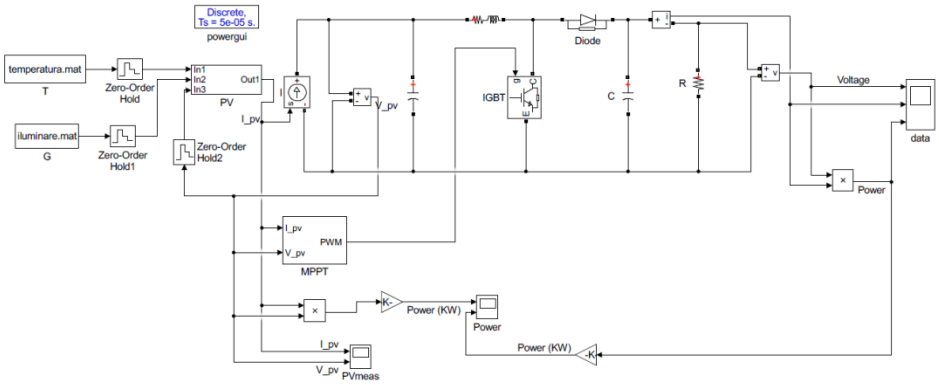

Fig.6. Primary scheme of the PV system and BOOST converter

Considering a maximum input current ripple limited to 5 A, a 10 mH BOOST converter coil is being chosen. Having a maximum equivalent DC load of 3 Ω and an output voltage ripple limited to 5 V, a 2 mF capacitor have been considered.

The BOOST converter IGBT command logic is illustrated in *Fig. 7*.

Voltage and current values are measured with a 0.1 ms sample. The algorithm calculates output power, following the output voltage and power variations of the PV system for each measurement sample. The IGBT PWM command is realized by comparing the modulation voltage wave with a control triangular voltage wave having an amplitude equal to 1 V and an 1250 Hz frequency. IGBT is switched on during the time the modulation voltage is higher than the control voltage.

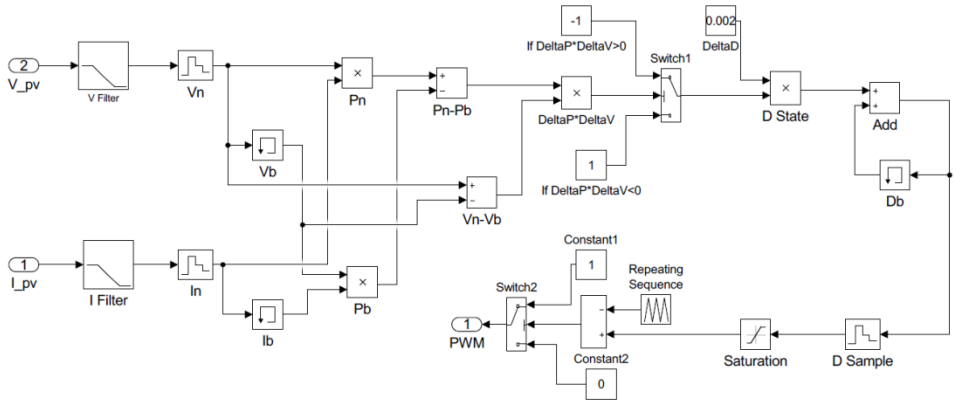

Fig.7. IGBT PWM command

Considering the fact that the first measured value of the PV system output voltage during this simulation is 0, it can be concluded that the starting regulation point on the *P-U* characteristic is represented by the short circuit condition. In case during a perturbation, the PV system output voltage and output power register variations in the same direction, the modulation voltage is decreased in order to obtain a lower switch on duration. The consequence of decreasing the switch on period is the diminution of the output current and the increase of the output voltage. In case during a perturbation power and voltage register variations in opposite directions, the modulation voltage is increased during the next perturbation step in order to obtain a higher switch on duration. The consequence of a higher switch on duration is the increase of the output voltage.

In order to keep the converter inside the stable operating area, the modulation voltage wave amplitude is limited to 0.8 V.

5. Simulation results

Considering the first measuring point of the characteristic day, the evolution of PV system output voltage and current is illustrated in *Fig. 8*. The PV system current ripple after maximum power point regulation convergence is below 5 A. The algorithm registers a complete operation during a time interval lower that 0.2 s.

Fig. 9 illustrated the evolution of PV system output power evolution during maximum power point tracking evolution.

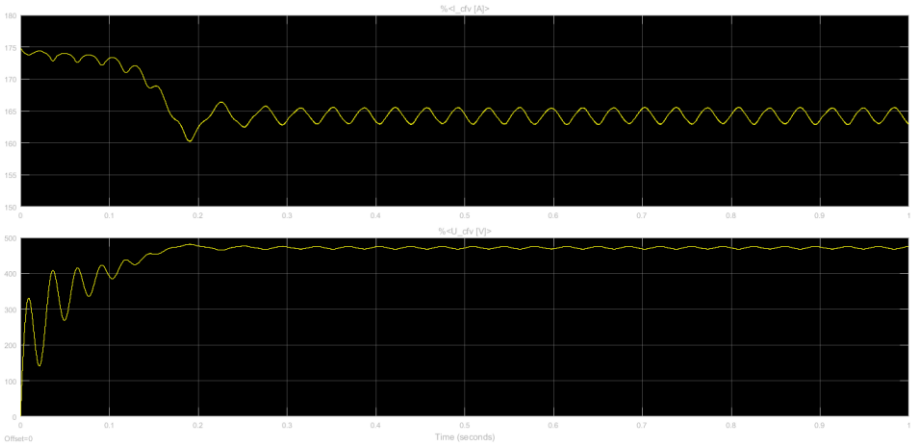

Fig.8. Output current and voltage evolution during maximum power point regulation

The upper graph follows power measured to the output connection of the PV system, while the graph situated below represents the evolution of power measured to the BOOST converter output connections. Small power ripple shown in the second graph is a consequence of the voltage ripple produced by IGBT switch operation.

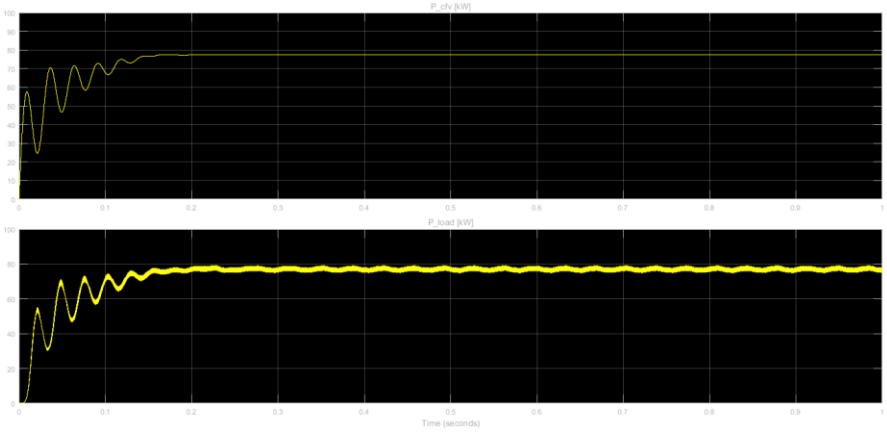

Fig.9. Output power evolution during maximum power point regulation

Taking into account the fact that the implemented algorithm speed of convergence is about 0.2 s, the drop-out time set for maintaining each measured value for temperature and solar irradiance during the characteristic day is set to 1 s. The variations of the output current and voltage are illustrated in *Fig. 10*. Fast solar irradiance variations have an important impact on P&O maximum power point regulation algorithm operation, observed by temporary deviations of the output voltage. However, steady-state voltage variations represent less than 20% of the maximum value. On the other hand, solar irradiance evolution during a variable nebulosity characteristic day generates important output current

variations. Temporary divergence is observed as short time voltage variations, representing drifts from the real maximum power point. The effects of this phenomenon are significantly reduced for IGBT switching frequencies higher than 1 kHz, as recovery is very fast in this situation.

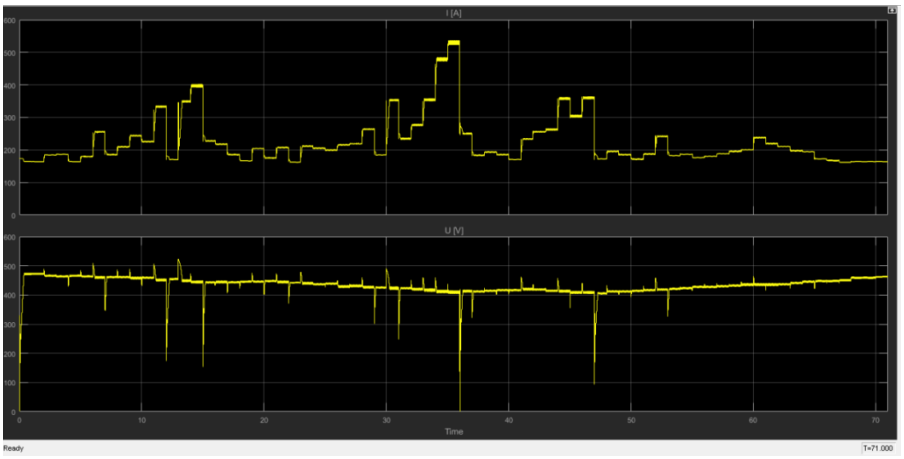

Fig.10. Output current and voltage variation during the characteristic day

Fig. 11 illustrates evolutions of output PV system power measured before and after the BOOST converter.

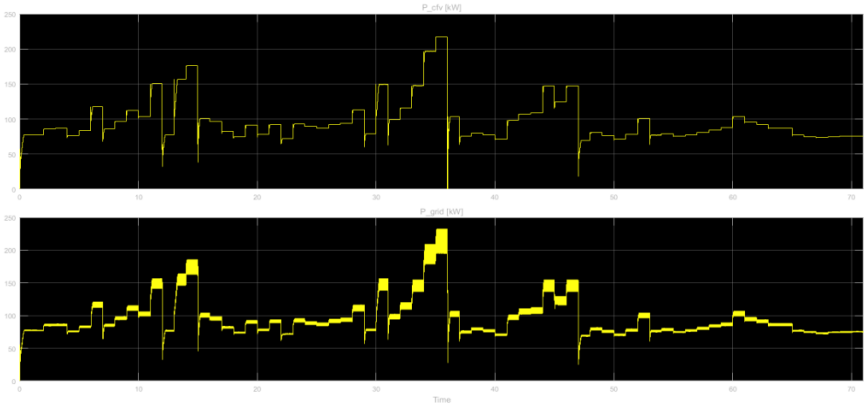

Fig.11. Output power variation during the characteristic day

5. Conclusions

Perturb and Observe maximum power point tracking algorithm has the major advantage of simple and economic implementation, eliminating the necessity of a distinct PLC in order to accomplish maximum power regulation function. On the other hand, the main disadvantage of P&O algorithm is represented by power losses during regulation and in steady state operation,

consequence of the permanent oscillation around the maximum power point. Furthermore, considering the case of fast solar irradiance variations, temporary divergence situations may occur.

Simulations performed during this work reveal that adequate dimensioning of the BOOST converter elements results in voltage and current ripple limitation and, implicitly, decrease of power losses in steady-state conditions. Considering fast variable solar irradiance conditions, it was concluded that a 1.25 kHz IGBT switching frequency provides a very fast convergence of the P&O algorithm, resulting in reduced energy losses during maximum power point regulation. Furthermore, another advantage of high IGBT switching frequency is represented by facile natural filtering of the BOOST converter output voltage waveform. The model designed during this work can be used for optimal tuning of any P&O maximum power point tracking regulator and BOOST converter element sizing, by performing comparative performance studies.

R E F E R E N C E S

[1]. *Sumedha Sengar*, "Maximum Power Point Tracking Algorithms for PV System: A Review", in International Review of Applied Engineering Research, **vol. 4**, no. 2, 2014, pp. 147-154

[2]. *Roberto Faranda, Sonia Leva*, "Energy comparison of MPPT techniques for PV Systems", in WSEAS Transactions on Power Systems, **vol. 3**, Issue 6, June 2008, pp. 446-455

[3]. *G. M. Tina, R. Abate*, "Experimental verification of thermal behavior of photovoltaic modules", in MELECON 2008- The 14th IEEE Mediterranean Electrotechnical Conference, no. 2, May 2008, pp. 579-584

[4]. *R. W. Erickson, D. Maksimovic*, Fundamentals of Power Electronics, Kluwer Academic Publishers, New York, 2004.

[5]. *J.A. Gow, C.D. Manning*, "Development of a photovoltaic array model for use in power electronics simulation models", IEEE Proceedings on Electric Power Applications, **vol. 146**, no.2, March 1999, pp. 192-200

[6]. *Th. Dănilă, N. Reus, V. Boiciu,* Dispozitive şi circuite electronice (Electronic circuits and devices), Editura didactică şi Pedagigică, Bucureşti 1982.

[7]. *I. Stamatescu, I. Făgărăşan, G. Stamatescu, N. Arghira, S.St. Iliescu*, "Design and Implementation of a Solar-tracking Algorithm", in Procedia Engineering, **vol. 69**, 2014, pp 500–507

[8]. *A.Pradeep Kumar Yadav, S.Thirumaliah, G.Haritha*, "Comparison of MPPT Algorithms for DC-DC Converters Based PV Systems", in International Journal of Advanced Research in Electrical, Electronics and Instrumentation Engineering, **vol. 1**, Issue 1, July 2012, pp. 18-23

[9]. *Chih-Lung Shen, Jye-Chau Su*, "Grid-Connection Single-Stage Photovoltaic Inverter System with Double-Linear-Approximation MPPT", in International Journal of Applied Mathematics and Information Sciences, **vol. 9**, No. 1L, February 2015, pp. 205-211

[10]. *Virgil Dumbrava, G.C. Lazaroiu, Sonia Leva, G. Balaban, Mihaela Teliceanu, Mihai Tirsu*, "Photovoltaic production management in stochastic optimized microgrids", U.P.B. Scientific Bulletin, Series C, **vol. 79**, Issue 1, 2017

[11]. *Mihaela Florentina Suchankova, Mihai Octavian Popescu*, "Modeling the consumption of a photovoltaic system", U.P.B. Scientific Bulletin, Series C, **vol. 78**, Issue 2, 2016.